

Article

Decoration of a Glass Surface with AgNPs Using Thio-Derivates for Environmental Applications

Cornelia-Ioana Ilie ^{1,2} , Angela Spoială ^{1,2} , Ludmila Motelica ^{1,2} , Liliana Marinescu ^{1,2}, Georgiana Dolete ^{1,2} , Doina-Roxana Truşcă ^{1,2}, Ovidiu-Cristian Oprea ^{3,4} , Denisa Ficai ⁴  and Anton Ficai ^{1,2,3,*} 

¹ Department of Science and Engineering of Oxide Materials and Nanomaterials, Faculty of Chemical Engineering and Biotechnologies, National University of Science and Technology POLITEHNICA Bucharest, 060042 Bucharest, Romania

² National Centre for Micro and Nanomaterials and National Centre for Food Safety, National University of Science and Technology POLITEHNICA Bucharest, 060042 Bucharest, Romania

³ Academy of Romanian Scientists, 050044 Bucharest, Romania

⁴ Department of Inorganic Chemistry, Physical Chemistry and Electrochemistry, Faculty of Chemical Engineering and Biotechnologies, National University of Science and Technology POLITEHNICA Bucharest, 060042 Bucharest, Romania

* Correspondence: anton.ficai@upb.ro

Abstract: The aim of this study is to decorate a glass surface with silver nanoparticles (AgNPs) and further prove its efficiency in the removal of some thio-derivatives—potential pollutants from water. Therefore, grafting the surface of glass-based platforms with AgNPs will strongly influence their interaction with other substances or molecules. The most commonly used molecules for glass-based platform functionalization/modification are organosilanes. In this case, the main interest is in thioalkyl organosilanes because, after silanization, the thio (-SH) functional groups that have a high affinity for AgNPs can intermediate their binding on the surface. By decorating the glass platforms with AgNPs, these surfaces become active for the adsorption of dyes from wastewater. Certainly, in this case, the dyes must bear -SH groups to ensure a high affinity for these surfaces. Therefore, the desired purpose of this study was to develop glass-based platforms decorated with AgNPs able to bind model molecules—dyes from aqueous media (dithizone—DIT and thioindigo—TIO), with these platforms being potentially used for environmental applications.

Keywords: glass surface silanization; organosilanes; silver nanoparticles; dyes removal; pollution



Citation: Ilie, C.-I.; Spoială, A.; Motelica, L.; Marinescu, L.; Dolete, G.; Truşcă, D.-R.; Oprea, O.-C.; Ficai, D.; Ficai, A. Decoration of a Glass Surface with AgNPs Using Thio-Derivates for Environmental Applications. *Coatings* **2024**, *14*, 96. <https://doi.org/10.3390/coatings14010096>

Academic Editor: Maria Jose Fabra

Received: 7 December 2023

Revised: 3 January 2024

Accepted: 8 January 2024

Published: 11 January 2024



Copyright: © 2024 by the authors. Licensee MDPI, Basel, Switzerland. This article is an open access article distributed under the terms and conditions of the Creative Commons Attribution (CC BY) license (<https://creativecommons.org/licenses/by/4.0/>).

1. Introduction

The fabrication of solid glass-based surfaces with silver nanoparticle (AgNPs) assemblies immobilized on their surfaces is currently of great importance because of the key role these substrates could play in developing various applications [1,2]. In this study, we have utilized the potential of glass-based platforms because they are economical, environmentally friendly, durable, reusable, and inert material, which has been demonstrated to be an excellent candidate in applications ranging from laboratory to industry [1,3]. The physicochemical properties of the obtained surfaces will depend on the size, shape, and surface features of the silver nanoparticles and the nature of the glass surfaces [4].

Normally, silver nanoparticles are attached to the glass surface/substrate through an intermediate layer of diverse molecules grafted on the surface. The grafting process is carried out with the help of the terminal functional groups due to their electrostatic or chemical interaction with the nanoparticles (NPs). The main characteristics of these surfaces/platforms are that they should be stable over time and their interaction with the NPs should be strong enough to ensure that the NPs continue to be attached to their surface during further functionalization [5,6].

The molecules commonly used for the functionalization of glass-based platforms are organosilanes, which are the most studied surface modifiers [7–9]. The affinity of the

glass for metal NPs involved functionalization with thiol alkyl silane as a silanizing agent because thio (-SH) groups have a high affinity for several metal nanoparticles including AgNPs. Likewise, the glass platforms with thiol alkyl silane decorated with AgNPs became active for the adsorption of thiol-derivates (amino acids, drugs, dyes, etc.) [10]. Moreover, the numerous studies dealing with the functionalization of glass surfaces with organosilanes have shown that the silanization step is very sensitive and important in terms of experimental conditions and that the final surface state of the modified substrate depends strongly on temperature, the presence of water, the concentration, and the duration of the grafting step [7].

Kawamura et al. [11] show that the decoration with a thin layer of 3-mercaptopropyltri methoxysilane (MPTMS) on the glass-based platform becomes electrically continuous, and due to the optical properties (transparency), these materials are suitable for semitransparent electrode devices. Likewise, another study presents the development (with the same self-assembling technique) of highly sensitive surface-enhanced Raman scattering (SERS) substrates with a limit of detection in the zeptomole for two dyes (Nile blue A and oxazine 720) [4]. Furthermore, the AgNPs-silanized glass platform can immobilize the adherence and growth of microorganisms on the surfaces because of direct contact with Ag⁺ ions (due to slow release) [5]. The antimicrobial capacity/activity of the developed glass platforms gives these materials the potential to have various applications (environmental, food packaging, biomedical, etc.) [6].

Alamier et al. [12] showed an effective green synthesis of AgNPs using *Acacia ehrenbergiana* plant extract for the efficient removal of Rhodamine B (RhB) dye. Besides the catalytic reductions, the antimicrobial activity of the obtained AgNPs was reflected in the novelty of the study. An interesting study carried out by Mokhtar et al. [13] illustrated the adsorption efficiency of AgNPs synthesized via *Clitoria ternatea* flower extract doped with activated carbon on the removal of RhB dye.

Furthermore, different studies regarding the exceptional catalytic and biological activity of AgNPs are presented. Other authors have shown that the AgNPs synthesized using *Plantago ovata* leaf extract had effectiveness in removing organic dyes (methylene blue and congo red) and antifungal activity [14].

The glass surface was modified with MPTMS and further used to generate Au and Ag nanostructures with different sizes and shapes (aspect ratio of 11 and 24, for the two kinds of nanoparticles) according to a seeding approach proposed by Lee et al. [15].

In this paper, glass-based platforms were obtained using MPTMS and MPTES/(3-mercaptopropyl) triethoxysilane as silanization agents for glass surface functionalization. Afterward, AgNPs-decorated glass platforms were obtained using AgNPs synthesized as decorating agents [16], by absorption. Moreover, these AgNPs-decorated surfaces were proved to be efficient in the absorption of thio-derivatives using two common dyes (such as dithizone and thioindigo), potential pollutants from aqueous solutions. Additionally, these dyes can be easily monitored by UV-Vis spectroscopy, and thus, their use is desirable.

2. Materials and Methods

2.1. Chemicals

The reagents isopropyl alcohol, NH₃ solution 25%, hydrogen peroxide 35%, HCl 37%, MPTMS, and MPTES were purchased from Sigma-Aldrich (Darmstadt, Germany). The dithizone was acquired from Chinoin (Ciudad de Mexico, Mexico), the thioindigo was from (TCI-Tokyo Chemical Industry Co., Tokyo, Japan), and the AgNPs used were synthesized and characterized according to previous studies [17,18]. The AgNPs used in this study were synthesized by the solvothermal method with polyethylene glycol as a reduction component, at 260 °C and 3 bar pressure for 1 h. The results in the case of the solvothermal reaction showed that the nanoparticles were spherical with an average size of 50 nm (HT4 synthesis from our previous paper [17]).

The microscope slides (26 × 76 mm, 1.0–1.2 mm thickness) were purchased from Labbox (Barcelona, Spain).

To descant upon this work, we studied the organic layer's influence on the decoration of AgNPs on functionalized glass-based platforms. Therefore, for this purpose, we explored the surface interaction, starting from the nature and features of the decorated glass-based platforms, as follows. In the first step, the pre-treatment of glass-based platforms with detergent and alcohol was performed [5]. Then, the first glass activation was conducted with a mixture of $\text{NH}_3/\text{H}_2\text{O}_2/\text{H}_2\text{O}$ (alkaline treatment). This stage was performed to introduce hydroxyl groups on the glass-based platforms and prepare the glass for the silanization process. The second glass activation was conducted with a mixture of $\text{HCl}/\text{H}_2\text{O}_2/\text{H}_2\text{O}$ (acid treatment). Then, the actual silanization occurs by treating the glass-based platforms with MPTMS and MPTES as silanization agents for the glass surface functionalization (Figure 1). As already mentioned, the main purpose for designing such glass is to identify diverse dyes presented in the polluted wastewater. Therefore, after decorating the glass surface with organosilanes, AgNPs were used to improve their properties and applicability for environmental applications. The obtained glass-based platforms were characterized by Fourier-transform infrared (FTIR) spectroscopy and microscopy, UV-Vis spectroscopy, and scanning electron microscopy (SEM).

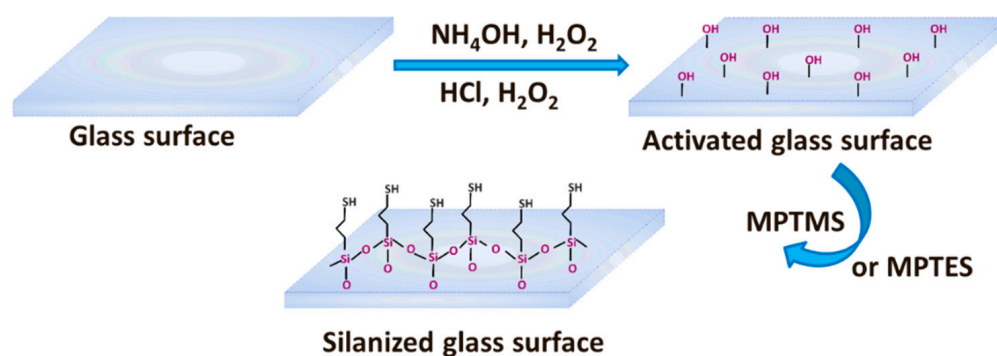


Figure 1. Glass surface functionalization procedure.

2.2. Cleaning Pre-Treatment

All glass samples were washed in an aqueous solution with detergent and rinsed with distilled water (DW) followed by cleaning with isopropyl alcohol. The slides were dipped in a mixture of NH_3 25%: H_2O_2 : H_2O = 1:1:5 (in volume) for 30 min (min) at 30 °C, followed by cleansing with DW, and treated with a mixture of HCl 37%: H_2O_2 : H_2O = 1:1:5 (in volume) for 30 min (min) at 85 °C. After these treatments, all samples were washed with DW, DW:isopropyl alcohol = 1:1, and isopropyl alcohol. The glass surface functionalization was immediately performed [16].

2.3. Glass Surface Modification

The glass-based platforms were performed using MPTMS and MPTES as thioalkyl silanization agents for the glass surface functionalization. All slides were immersed in a 1, 3, and 5% MPTMS/MPTES (*v:v*) alcoholic solution at 30 °C, 25 rpm for 24 h. The silanization agent excess was washed with isopropyl alcohol, isopropyl alcohol:WD = 1:1, WD, and dried at room temperature. All treatments were performed using tightly closed PVC centrifuge tubes [16].

2.4. Decoration with AgNPs of Silanized Glass Platforms

In the second step, glass platforms were decorated using AgNPs. All samples were immersed in 1.2 ppm AgNPs solution at room temperature and 20 rpm for 10 days. The adsorption of AgNPs was followed by measurements at 405 nm using a UV-Vis spectrophotometer. AgNP quantification was performed using a six-point calibration curve covering

the 0.08–1.2 ppm range. The AgNPs deposited (mg/m^2) were calculated according to the calibration curve ($y = mx + b$) and using the following equation (Equation (1)):

$$\mu\text{g substance deposited} = \frac{(A_i - A_f) - b}{\frac{m \times \text{Volume}}{\text{Glass surface area}}} \quad (1)$$

A_i —absorbance, initial, A_f —absorbance, final, b —constant, m —glass mass, and the volume of glass immersion.

2.5. Adsorption of Dyes to AgNPs-Decorated Glass Platforms

Additionally, to improve the properties and applicability of the AgNPs-decorated glass platforms, DIT and TIO were used as standard dyes for testing the removal capacity. The AgNPs-decorated slides were immersed in 10 ng/mL DIT solution at room temperature and 25 rpm for 4 days. The adsorption of DIT was followed by spectrophotometric measurements at 595 nm. DIT quantification was performed using a six-point calibration curve covering the 0.75–10 ng/mL range.

The TIO decoration was performed using the same steps with a 20 ng/mL solution (in ethanol) and measured at 453, 459, and 540 nm. The spectrophotometric measurements were performed at six specific wavelengths, but of these, only the values in the visible range were retained because the values in the UV range were not conclusive; there are complex processes of Ag^+ ion release and TIO absorption (natural and degraded). Likewise, the experimental wavenumbers 453, 459, and 540 nm are specifically for *trans*-thioindigo isomers [19,20].

The dyes deposited ($\mu\text{g}/\text{m}^2$) on the AgNPs-decorated glass platforms were also calculated using Equation (1).

2.6. Characterization Methods

The obtained glass-based platforms were characterized by FTIR spectroscopy and microscopy, UV-Vis spectroscopy, and scanning electron microscopy (SEM).

The FTIR spectra were recorded with a Nicolet iS50 FTIR spectrometer (Thermo Fisher Scientific, Waltham, MA, USA), using the attenuated total reflection accessory (ATR) (Thermo Fisher Scientific, Waltham, MA, USA). All spectra were obtained as an average of 32 scans over the spectral range of 400–4000 cm^{-1} at a resolution of 4 cm^{-1} . FTIR 2D maps were obtained with a Nicolet iN10 MX FTIR microscope, equipped with a DTGS detector, between 600 and 4000 cm^{-1} . Information about the spatial distribution of the components was extracted from the 2D FTIR maps [21].

The UV-Vis Evolution 300 spectrophotometer (Thermo Fisher Scientific, Waltham, MA, USA) includes a long-lifetime xenon flash lamp and a silicon photodiode detector with extended wavelength ranging up to 900 nm. Moreover, the equipment includes photo-etched slits for greater accuracy and a stepper-motor-driven slit drive with intelligent optimization. The grating features are 1200 lines/mm, 240 nm blazed, holographic grating for exceptional stray light performance. Also, the spectrophotometer 4.5.0 VisionPro software, which offers advanced scanning, multiple fixed wavelength measurements, and multi-wavelength measurements with customized UVcalc [22].

The morphology of the glass-based platforms samples was investigated by scanning electron microscopy (SEM) using a high-resolution microscope Quanta 250 (FEI Company, Eindhoven, The Netherlands), incorporated with an energy dispersive X-ray spectrometer, produced by EDAX (Mahwah, NJ, USA), consisting of Element EDS Analysis EDX GENESIS XM4 Software (Mahwah, NJ, USA) [23]. For sample preparation, a small amount of each sample was fixed on the carbon SEM stub that was placed inside of the analysis chamber, resulting in a sample covered with a 10 nm gold layer [21].

3. Results and Discussion

3.1. FTIR Microscopy and Spectroscopy

3.1.1. Characterization of Glass-Silanized and AgNPs-Decorated Platforms

Characterization of the MPTMS- and MPTEs-silanized platforms using FTIR spectroscopy and microscopy is shown in Figures 2 and 3.

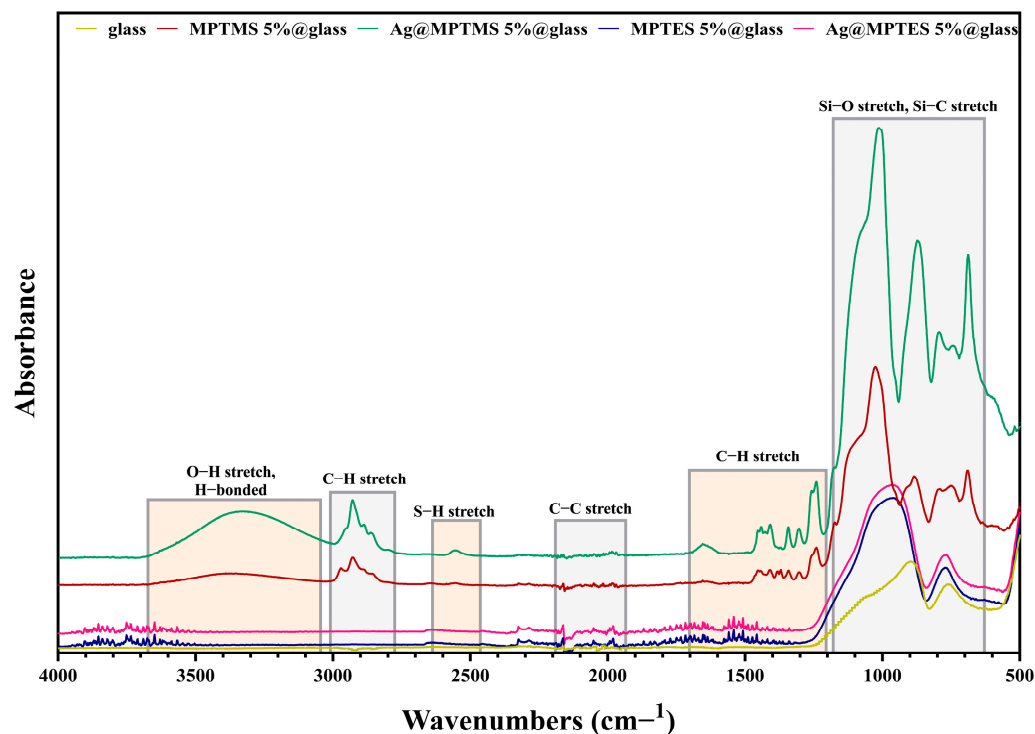


Figure 2. FTIR spectra for glass and glass-based platforms silanized with MPTMS and MPTEs and their derived AgNPs-decorated glass surfaces.

Figure 3 presents FTIR maps related to the MPTMS/MPTEs-silanized glass platforms (1, 3 and 5%) and shows the most representative peaks, recorded at the wavelength's characteristic of Si-C, Si-O, C-H, S-H, $-\text{CH}_2$, and $-\text{CH}_3$ (812 , 1272 , $1342/1344$, $2561/2566$, $2837/2886$, and $2940/2974$ cm^{-1}) [8]. Thus, one can observe visible similarities between the FTIR diagrams related to the glass surfaces/platforms silanized with MPTEs and MPTMS and at the same time an adequate, homogeneous functionalization of the surface.

In the maps above, similarities can be seen as follows: in the case of MPTMS-silanized surfaces, the following vibration bands at 2940 and 2837 cm^{-1} , characteristic of the C-H functional bond (asymmetric and symmetric), were observed. C-H bonds were also present at 1344 cm^{-1} , as well as the S-H bond at 2561 cm^{-1} . Very important to illustrate are the peaks at 812 cm^{-1} and 1272 cm^{-1} , which were confirmed by the presence of the Si-C and Si-O bond (glass) [24].

In the case of glass platforms silanized with MPTEs, 2974 and 2886 cm^{-1} are characteristic of the C-H functional bond (asymmetric and symmetric). Likewise, the presence of C-H deformation vibrations at 1342 cm^{-1} can be observed, as well as S-H stretching vibrations from 2566 cm^{-1} . As in the previous case, we have the peaks at 812 cm^{-1} and 1272 cm^{-1} , which were confirmed by the presence of the Si-C functional bond (glass) [25–27].

Recent studies include numerous works regarding the interaction of various metals (Au, Ag, or Cu) with the “-SH” functional group, which is why MPTMS and MPTEs are used as precursors in the preparation of silanized/functionalized surfaces with mercaptopropyl moieties for “capturing” noble metal nanoparticles [15,28–30].

In the case of the glass platforms silanized with thiol alkyl silanes (Figure 2) and decorated with AgNPs (Figure 4), the presence of the same bands characteristic of each

functional group related to the glass samples silanized with MPTMS and MP TES can be observed. Thus, in the case of the glass platforms silanized with AgNPs@MPTMS (1, 3, and 5%), as well as those silanized with AgNPs@MP TES (1, 3, and 5%), the FTIR maps show visible similarities, which proves the good homogeneity of the samples/functionalization of the glass platforms [27,31,32].

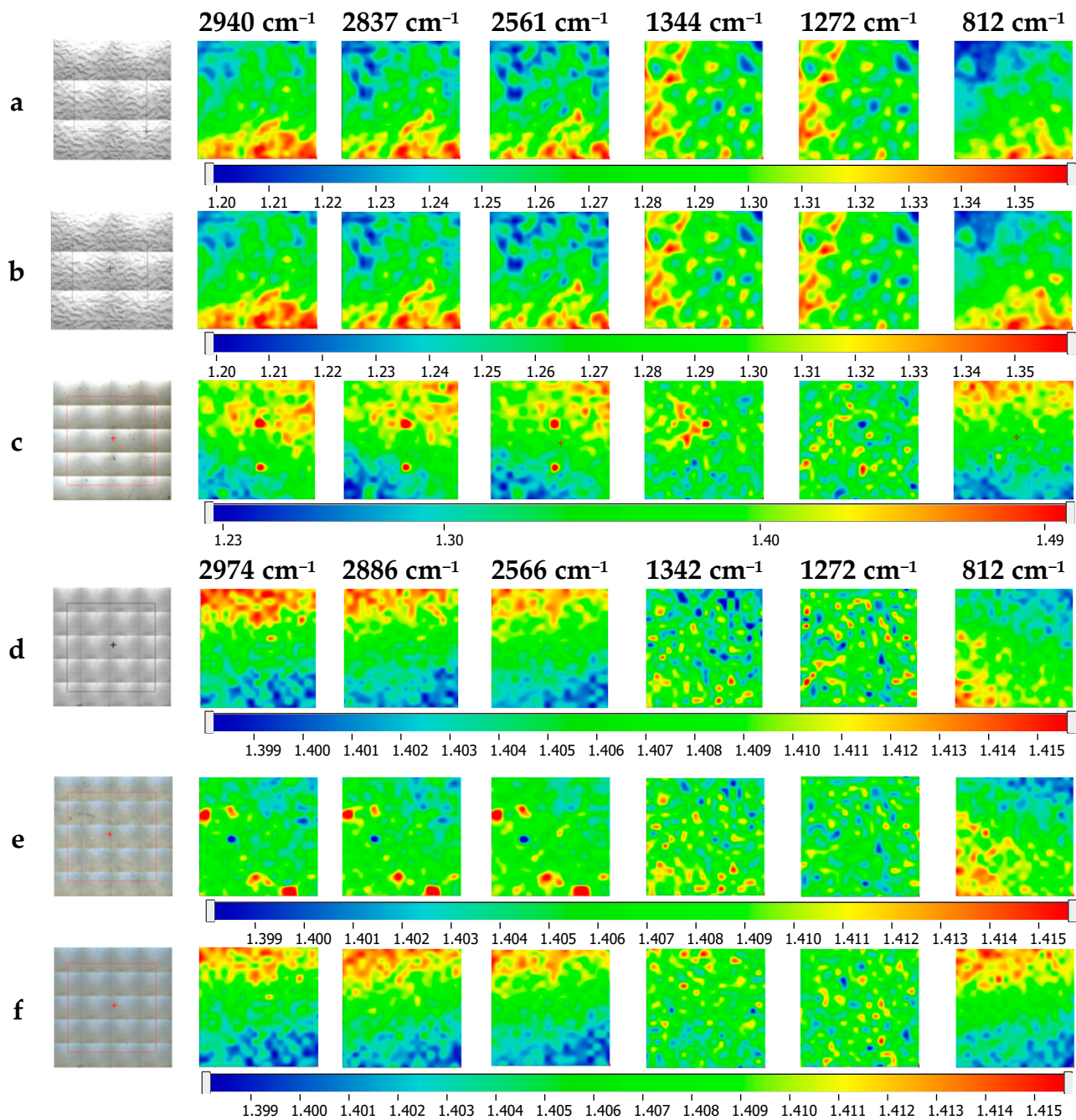


Figure 3. FTIR maps for glass-silanized platforms. (a) MPTMS 1%, (b) MPTMS 3%, (c) MPTMS 5%, (d) MP TES 1%, (e) MP TES 3%, and (f) MP TES 5%; in all cases, the scanned surfaces were of $600 \mu\text{m} \times 600 \mu\text{m}$.

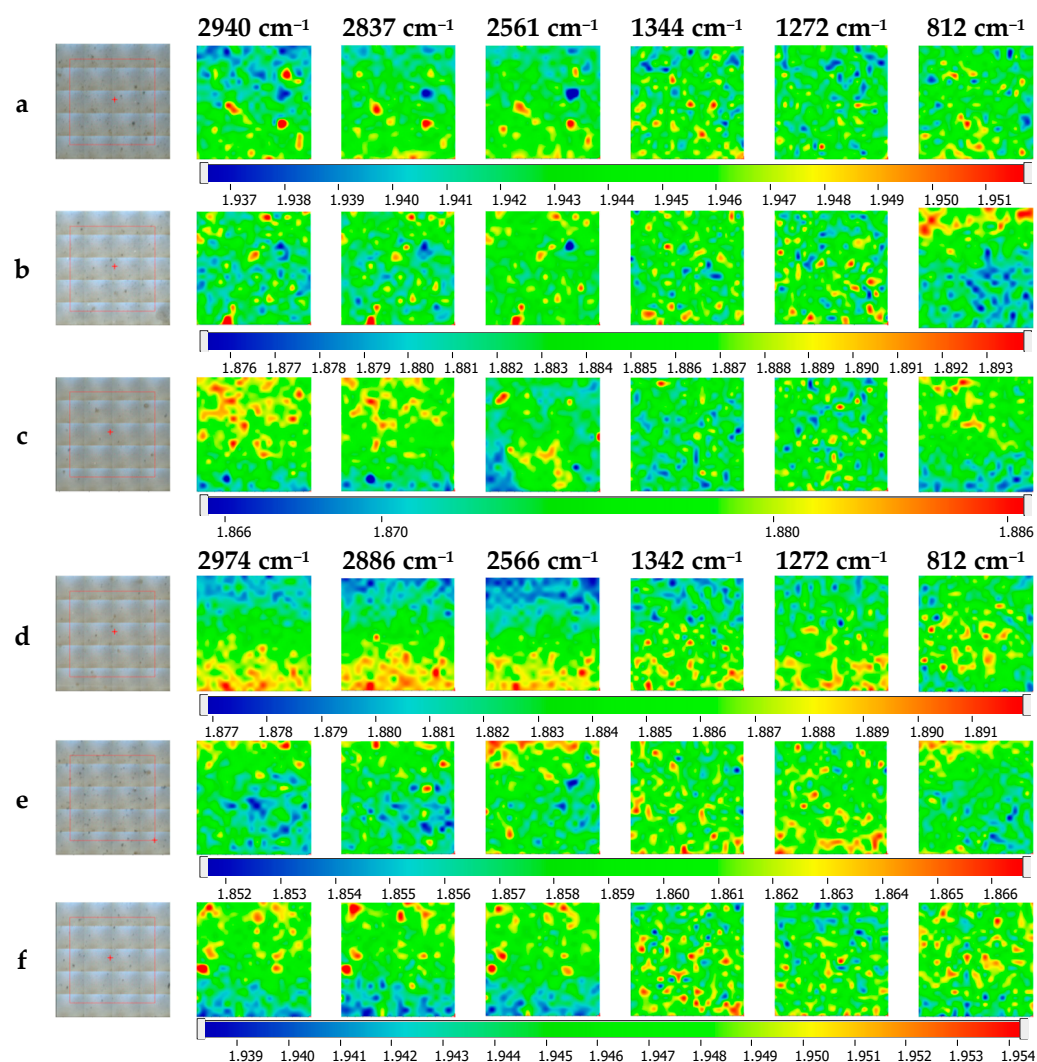


Figure 4. FTIR maps for AgNPs-decorated glass platforms. (a) AgNPs@MPTMS 1%, (b) AgNPs@MPTMS 3%, (c) AgNPs@MPTMS 5%, (d) AgNPs@MPTES 1%, (e) AgNPs@MPTES 3%, and (f) AgNPs@MPTES 5%; in all cases, the scanned surfaces were of $1400 \mu\text{m} \times 1400 \mu\text{m}$.

3.1.2. Characterization of Ag-Decorated Glass Platforms from the Point of View of Their Dye Retention

The adsorption of pollutants is a technique used in the capture of numerous compounds found in wastewater and polluted environments. This adsorption is desired in order to ensure not only removal from the environment but also for sampling purposes, and according to the sampling conditions, the sorbents can be used to determine the real concentration of the pollutants from the environment. Coal is most often used, but its reusability is low, and it cannot be used for the direct determination of the concentration of the pollutants [33].

Next, the characterizations of the glass platforms silanized and decorated with DIT and TIO are presented.

In Figure 5, the maps belonging to the glass surfaces decorated with AgNPs after exposure to the DIT are presented. It is worth mentioning that these maps were recorded at the main peaks/bands characteristic of the functional groups related to silanized glass slides decorated with AgNPs and exposed to DIT solution. According to the illustrated images and the color intensity grid, a uniformity of DIT deposition on the surfaces of the glass slides is also observed in these samples. In addition to Figures 3 and 4, the FTIR maps of the main DIT functional groups are shown: N-H (3437 cm^{-1}), S-H ($2600\text{--}2550 \text{ cm}^{-1}$), etc. [34,35].

In Figure 6, the maps with the most representative adsorption bands related to TIO are illustrated. Thus, between 3070 and 3190 cm^{-1} , the C-H (aromatic) functional bond is present. Also, present are the adsorption bands of the functional bond C=O between 1600 and 1700 cm^{-1} , C=C between 1590 and 1630 cm^{-1} , and C-H between 1080 and 1140 cm^{-1} , as well as adsorption bands from 961 cm^{-1} related to the C-S functional bond [36].

The presented microscopy analyses demonstrate the homogeneous adsorption of the dyes over the AgNPs-decorated glass slides via the MPTMS or MP TES linker.

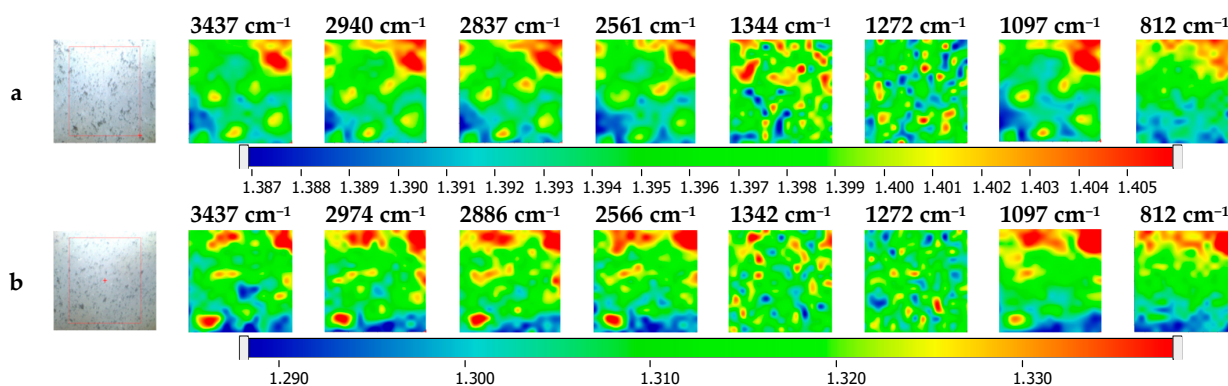


Figure 5. FTIR maps recorded on the AgNPs-decorated glass platforms after exposure to DIT. (a) DIT@AgNPs@MPTMS 5% and (b) DIT@AgNPs@MP TES 5%; in all cases, the scanned surfaces were of 350 $\mu\text{m} \times 350 \mu\text{m}$.

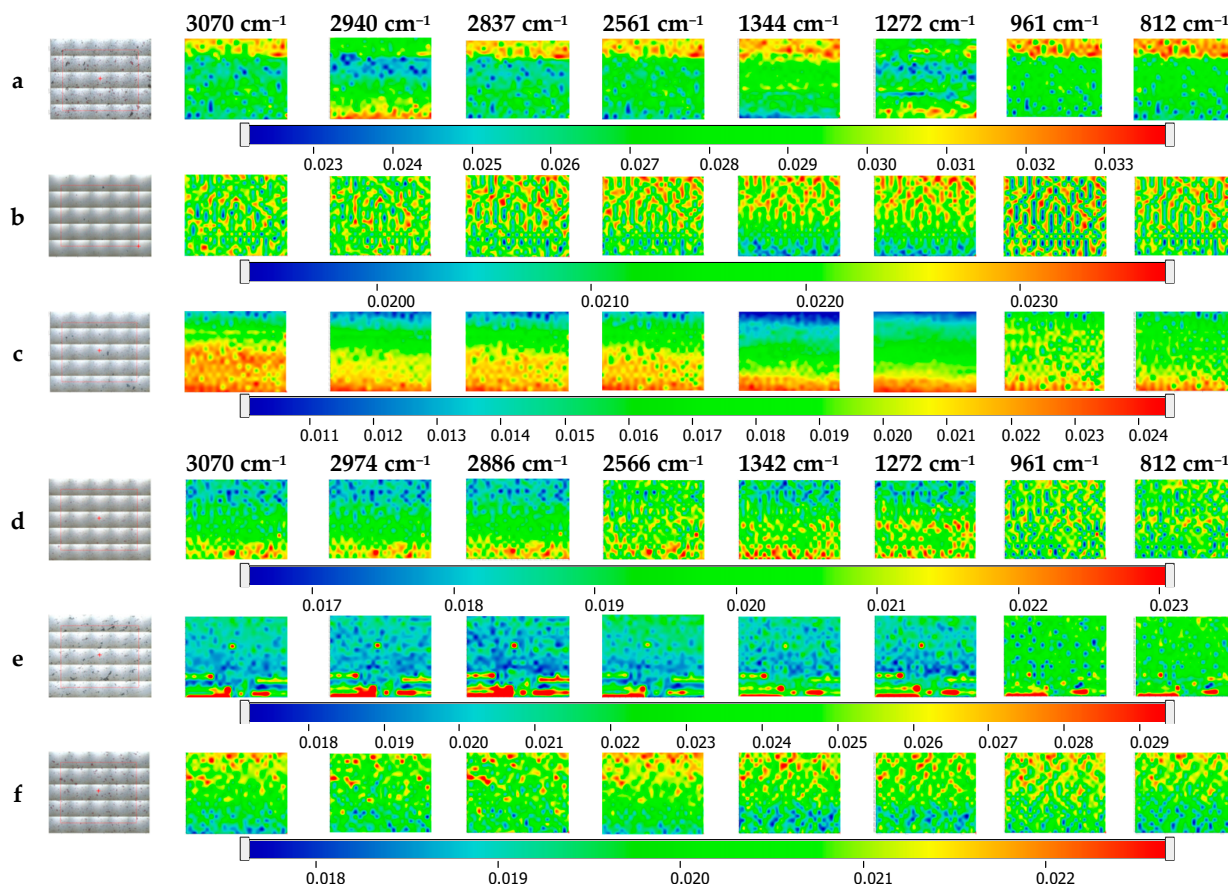


Figure 6. FTIR maps for thioindigo- and AgNPs-decorated glass platforms. (a) TIO@AgNPs@MPTMS 1%, (b) TIO@AgNPs@MPTMS 3%, (c) TIO@AgNPs@MPTMS 5%, (d) TIO@AgNPs@MP TES 1%, (e) TIO@AgNPs@MP TES 3%, and (f) TIO@AgNPs@MP TES 5%; in all cases, the scanned surfaces were of 1800 $\mu\text{m} \times 1400 \mu\text{m}$ (xy).

3.2. UV-Vis Spectroscopy

3.2.1. Decoration with AgNPs of the MPTMS/MP TES-Silanized Glass Platforms

Since “-SH” groups have a high affinity for AgNPs [32], the “-alkylated” glass slides decorated with AgNPs are expected to be suitable for the binding of thio-derivatives including dyes.

The adsorption and affinity of AgNPs depending on the silanization agent used are shown in Figure 7. In the case of the glass platforms silanized with MPTMS (graph “a”), a greater quantity of deposited Ag is observed compared to those with MP TES. Also, the affinity of AgNPs increased with increasing silanizing agent concentration, and the platforms with 3 and 5% MPTMS/MP TES present the highest amounts of adsorbed AgNPs.

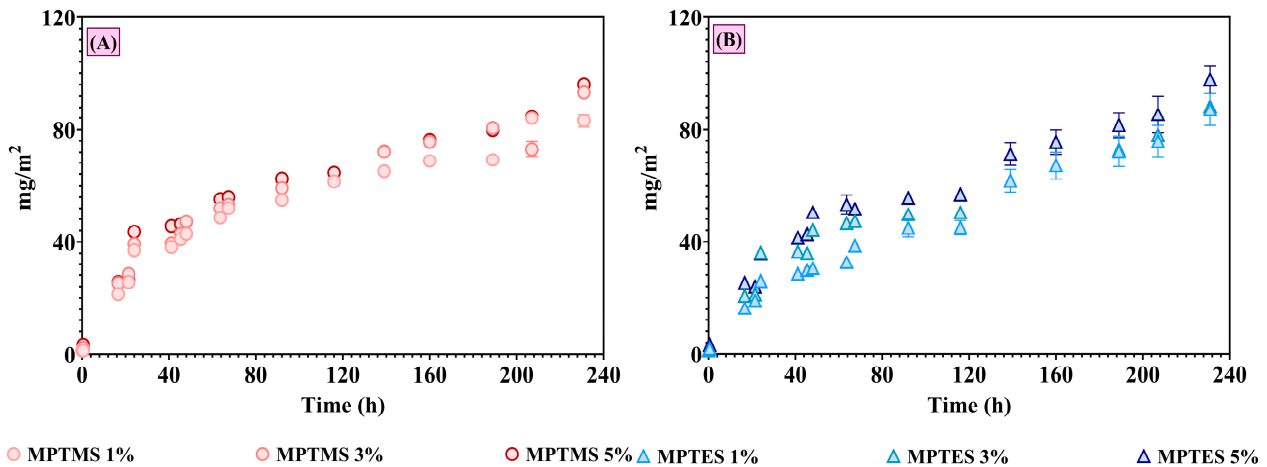


Figure 7. AgNPs-decorated on the silanized glass platform over time. (A)—AgNPs@MPTMS glass-decorated platform and (B)—AgNPs@MP TES glass-decorated platform.

3.2.2. Adsorption of Dyes to Ag-Glass-Decorated Platforms

Glass platforms silanized with MPTMS and MP TES and decorated with Ag nanoparticles became active for the adsorption of thiol-derivatives (dyes, amino acids, drugs, etc.) [37]. Addressing the critical issue of environmental pollution and the requirement to remove hazardous dyes from wastewater [38], two dyes were studied: dithizone and thioindigo.

In the case of the adsorption of DIT on the surface of the AgNPs-decorated silanized glass platforms (Figure 8), it can be observed that, with time, DIT adsorbed more on the surface of the AgNPs-decorated glass platforms silanized with MPTMS/MP TES 5%.

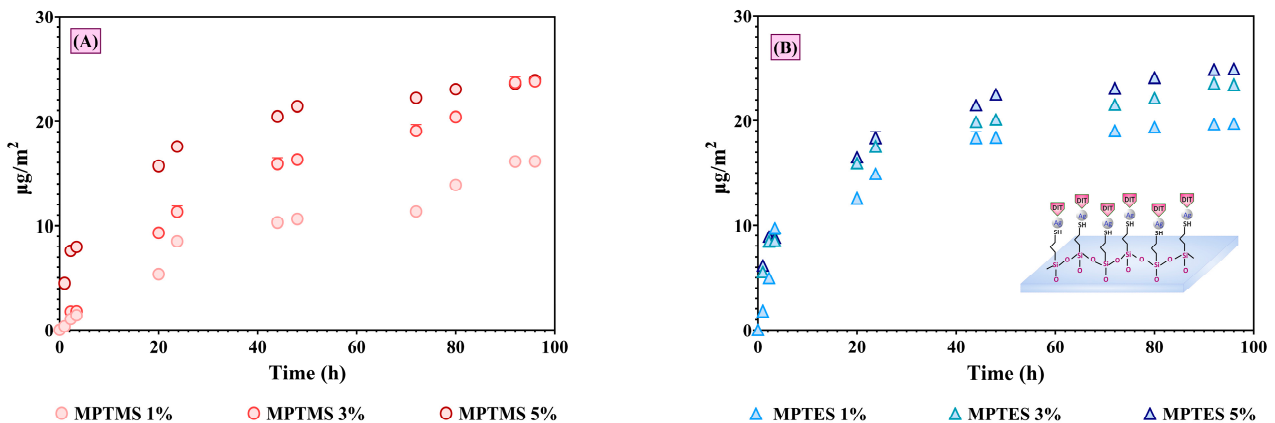


Figure 8. Dithizone adsorbed onto the AgNPs-decorated silanized glass platforms over time. (A)—DIT@AgNPs@MPTMS glass-decorated platform and (B)—DIT@AgNPs@MP TES glass-decorated platform.

The evaluation of the TIO adsorption on the AgNPs-decorated silanized glass surface was performed at three wavelengths: 453, 459, and 540 nm (Figure 9). From the following graphs, it was observed that at all three wavelengths, TIO adsorbed the most on glass surfaces silanized with 1% MPTMS/MP TES followed by 3 and 5%.

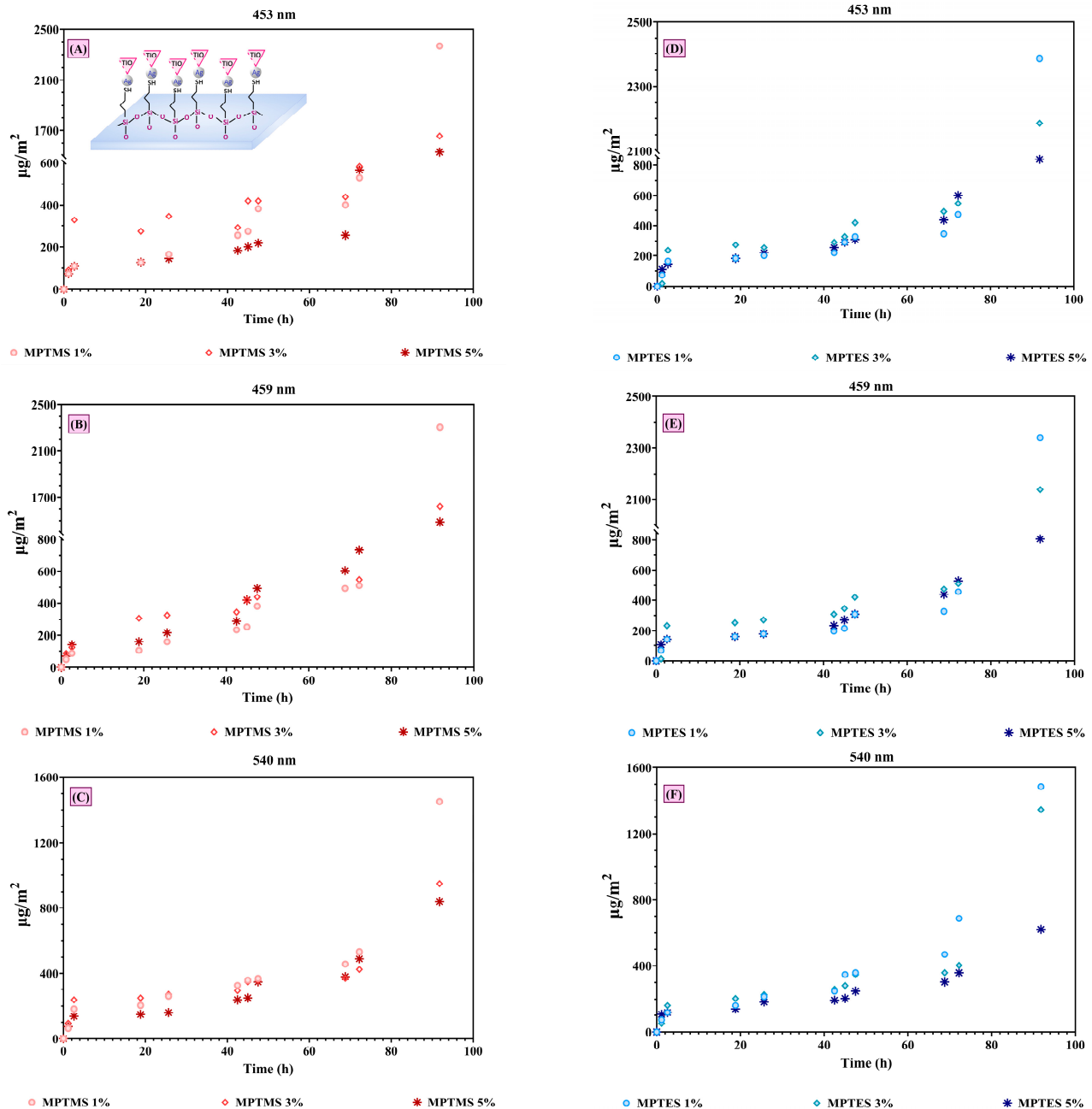


Figure 9. Thioindigo adsorbed onto the AgNPs-decorated silanized glass platforms. (A,D)—absorption of TIO at 453 nm; (B,E)—absorption of TIO at 459 nm; (C,F)—absorption of TIO at 540 nm.

Even over a short absorption time, TIO is absorbed better compared to DIT, with the experimental data showing absorption of 100–500 $\mu\text{g}/\text{m}^2$ (20–60 min). Moreover, DIT is adsorbed at ~ 24 – 25 $\mu\text{g}/\text{m}^2$ compared with the TIO, which can reach 2300 $\mu\text{g}/\text{m}^2$ if the evaluation is performed based on the data at 453 or 459 cm^{-1} or ~ 1500 $\mu\text{g}/\text{m}^2$ if the evaluation is performed based on the data at 540 cm^{-1} . The huge difference between these data can be explained most probably because of the different absorption of the TIO-related species from the solution. More research will be necessary to clarify this result through chromatographic assessments.

The interaction between DIT and TIO with the AgNPs-decorated silanized glass platforms developed in this study is due to the MPTMS/MP TES, which induces the coupling reaction of thiols [16]. Likewise, the AgNPs present an affinity for dyes. For example, the self-assembled monolayers of Prussian blue were grafted onto the Ag-decorated silanized glass surfaces [39].

3.3. SEM

Figure 10 shows the SEM images for silanized glass platforms decorated with AgNPs and dyes (DIT and TIO).

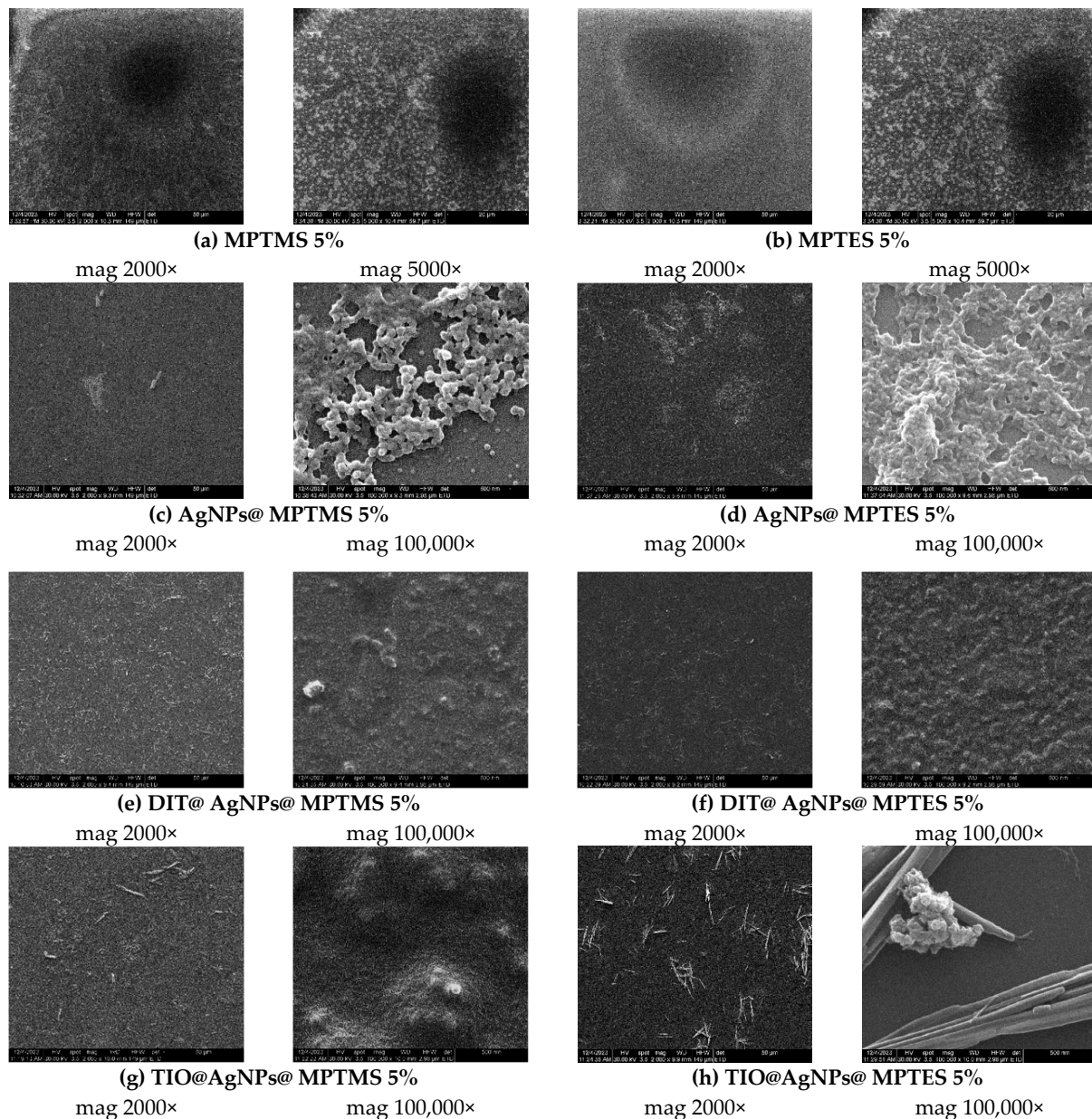


Figure 10. Representative SEM images of the glass platforms modified with: (a) MPTMS 5% and (b) MP TES 5%; (c) MPTMS 5% and decorated with AgNPs; (d) MP TES 5% and decorated with AgNPs; (e) MPTMS 5% and decorated with AgNPs after the adsorption of DIT; (f) MP TES 5% and decorated with AgNPs after the adsorption of DIT; (g) MPTMS 5% and decorated with AgNPs after the adsorption of TIO; and (h) MP TES 5% and decorated with AgNPs after the adsorption of TIO.

From the glass-based platforms silanized with MPTMS/MP TES 5% (Figure 10a,b), the smooth surface of the glass platforms can be observed. Instead, on the glass-based platforms

decorated with AgNPs@MPTMS/MPTES 5% (Figure 10c,d), at 100,000 \times magnification, it can be observed that on the platform's surface, AgNPs were deposited. This fact indicates that Ag bonded with the thio-alkyl chain through -SH functional groups that are well known to have a high affinity for AgNPs.

On the other hand, both samples exposed to the two dyes: DIT (Figure 10e,f) and TIO (Figure 10g,h) appear highly different in the SEM images compared with the AgNPs-decorated silanized glass platforms. Therefore, by comparison, the two systems denoted as TIO@AgNPs@MPTES 5% and DIT@AgNPs@MPTES 5% can observe different shapes, which is most probably because of the deposition of the dyes mediated by the presence of AgNPs.

4. Conclusions

In this work, we proved the ability of a glass surface to bind thio-derivatives (two dyes, namely thioindigo and dithizone). This affinity for such thio-derivatives was generated by a two-step surface modification of the glass which first involves functionalization by covalently bonded thioalkyl chains on the glass surface followed by decoration with AgNPs, which are adsorbed because of the high affinity of the thioalkylated surface to such nanoparticles. Based on these results, we can observe an important difference in the adsorption capacity of these surfaces to the two dyes, 24–25 $\mu\text{g}/\text{m}^2$ for dithizone and ~ 2300 $\mu\text{g}/\text{m}^2$ for thioindigo. Based on these results, further work will be conducted in order to evaluate the potential applications of these modified glass slides for specific applications in pollutant removal (thio-derivatives) or just for sampling or diagnosis (rapid diagnosis of the presence of dyes in aqueous media).

Author Contributions: Conceptualization, C.-I.I., D.F. and A.F.; Methodology, C.-I.I., A.S., O.-C.O. and A.F.; Software, C.-I.I. and G.D.; Validation, A.S.; Formal analysis, C.-I.I., A.S., L.M. (Ludmila Motelica), L.M. (Liliana Marinescu) and D.-R.T.; Investigation, L.M. (Ludmila Motelica); Resources, L.M. (Liliana Marinescu); Data curation, G.D. and D.F.; Writing—original draft, C.-I.I. and A.S.; Writing—review & editing, C.-I.I., G.D. and D.F.; Visualization, O.-C.O. and D.F.; Supervision, O.-C.O. and A.F.; Project administration, A.F. All authors have read and agreed to the published version of the manuscript.

Funding: The APC was funded by UNSTPB.

Institutional Review Board Statement: Not applicable.

Informed Consent Statement: Not applicable.

Data Availability Statement: Data are contained within the article.

Acknowledgments: The authors acknowledge the financial support of the “Functionalization and decoration with nanoparticles of the glass surface. A promising approach to inducing new applications”-PN-III-P1-1.1-TE-2021-1242, Ctr. No. TE95/2022, and the National Centre for Micro and Nanomaterials.

Conflicts of Interest: The authors declare no conflict of interest.

References

1. Majhi, S.; Sharma, K.; Singh, R.; Ali, M.; Tripathi, C.S.P.; Guin, D. Development of Silver Nanoparticles Decorated on Functional Glass Slide as Highly Efficient and Recyclable Dip Catalyst. *Chemistryselect* **2020**, *5*, 12365–12370. [[CrossRef](#)]
2. Badan, J.A.; Navarrete-Astorga, E.; Henriquez, R.; Jimenez, F.M.; Ariosa, D.; Ramos-Barrado, J.R.; Dalchiele, E.A. Silver Nanoparticle Arrays onto Glass Substrates Obtained by Solid-State Thermal Dewetting: A Morphological, Structural and Surface Chemical Study. *Nanomaterials* **2022**, *12*, 617. [[CrossRef](#)]
3. Barman, B.; Dhasmana, H.; Verma, A.; Kumar, A.; Singh, D.N.; Jain, V.K. Fabrication of silver nanoparticles on glass substrate using low-temperature rapid thermal annealing. *Energy Environ.* **2018**, *29*, 358–371. [[CrossRef](#)]
4. Fan, M.; Brolo, A.G. Silver nanoparticles self assembly as SERS substrates with near single molecule detection limit. *Phys. Chem. Chem. Phys.* **2009**, *11*, 7348–7349. [[CrossRef](#)] [[PubMed](#)]
5. Pallavicini, P.; Taglietti, A.; Dacarro, G.; Diaz-Fernandez, Y.A.; Galli, M.; Grisoli, P.; Patrini, M.; Santucci De Magistris, G.; Zaroni, R. Self-assembled monolayers of silver nanoparticles firmly grafted on glass surfaces: Low Ag⁺ release for an efficient antibacterial activity. *J. Colloid. Interface Sci.* **2010**, *350*, 110–116. [[CrossRef](#)]

6. Barzan, G.; Rocchetti, L.; Portesi, C.; Pellegrino, F.; Taglietti, A.; Rossi, A.M.; Giovannozzi, A.M. Surface Minimal Bactericidal Concentration: A comparative study of active glasses functionalized with different-sized silver nanoparticles. *Colloids Surf. B Biointerfaces* **2021**, *204*, 111800. [[CrossRef](#)]
7. Aissaoui, N.; Bergaoui, L.; Landoulsi, J.; Lambert, J.F.; Boujday, S. Silane layers on silicon surfaces: Mechanism of interaction, stability, and influence on protein adsorption. *Langmuir* **2012**, *28*, 656–665. [[CrossRef](#)]
8. Chen, J.J.; Struk, K.N.; Brennan, A.B. Surface modification of silicate glass using 3-(mercaptopropyl)trimethoxysilane for thiol-ene polymerization. *Langmuir* **2011**, *27*, 13754–13761. [[CrossRef](#)]
9. Ploetz, E.; Visser, B.; Slingenberg, W.; Evers, K.; Martinez-Martinez, D.; Pei, Y.T.; Feringa, B.L.; De Hosson, J.T.M.; Cordes, T.; van Dorp, W.F. Selective functionalization of patterned glass surfaces. *J. Mater. Chem. B* **2014**, *2*, 2606–2615. [[CrossRef](#)]
10. Wu, Y.; Song, Y.; Wu, D.; Mao, X.; Yang, X.; Jiang, S.; Zhang, C.; Guo, R. Recent Progress in Modifications, Properties, and Practical Applications of Glass Fiber. *Molecules* **2023**, *28*, 2466. [[CrossRef](#)]
11. Kawamura, M.; Fudei, T.; Abe, Y. Growth of Ag thin films on glass substrates with a 3-mercaptopropyltrimethoxysilane (MPTMS) interlayer. *J. Phys. Conf. Ser.* **2013**, *417*, 012004. [[CrossRef](#)]
12. Alamier, W.M.; Oteef, M.D.Y.; Bakry, A.M.; Hasan, N.; Ismail, K.S.; Awad, F.S. Green Synthesis of Silver Nanoparticles Using Acacia ehrenbergiana Plant Cortex Extract for Efficient Removal of Rhodamine B Cationic Dye from Wastewater and the Evaluation of Antimicrobial Activity. *Acs Omega* **2023**, *8*, 18901–18914. [[CrossRef](#)] [[PubMed](#)]
13. Mokhtar, M.A.M.; Ali, R.R.; Isa, E.D.M.; Tarmizi, Z.I.; Zhe, J.C.; Kasmani, R.M.; Yunos, D.D.M. Green synthesis of silver nanoparticles doped activated carbon for Rhodamine B dye adsorption. In *Journal of Physics: Conference Series, Proceedings of the 9th Conference on Emerging Energy & Process Technology, Johor Bahru, Malaysia, 24–25 November 2021*; IOP Publishing: Bristol, UK, 2022; pp. 1–8.
14. Githala, C.K.; Raj, S.; Dhaka, A.; Mali, S.C.; Trivedi, R. Phyto-fabrication of silver nanoparticles and their catalytic dye degradation and antifungal efficacy. *Front. Chem.* **2022**, *10*, 994721. [[CrossRef](#)] [[PubMed](#)]
15. Lee, K.-H.; Huang, K.-M.; Tseng, W.-L.; Chiu, T.-C.; Lin, Y.-W.; Chang, H.-T. Manipulation of the Growth of Gold and Silver Nanomaterials on Glass by Seeding Approach. *Langmuir* **2007**, *23*, 1435–1442. [[CrossRef](#)] [[PubMed](#)]
16. Pallavicini, P.; Dacarro, G.; Galli, M.; Patrini, M. Spectroscopic evaluation of surface functionalization efficiency in the preparation of mercaptopropyltrimethoxysilane self-assembled monolayers on glass. *J. Colloid Interface Sci.* **2009**, *332*, 432–438. [[CrossRef](#)] [[PubMed](#)]
17. Marinescu, L.; Ficaï, D.; Ficaï, A.; Oprea, O.; Nicoara, A.I.; Vasile, B.S.; Boanta, L.; Marin, A.; Andronescu, E.; Holban, A.M. Comparative Antimicrobial Activity of Silver Nanoparticles Obtained by Wet Chemical Reduction and Solvothermal Methods. *Int. J. Mol. Sci.* **2022**, *23*, 5982. [[CrossRef](#)] [[PubMed](#)]
18. Gheorghe-Barbu, I.; Corbu, V.M.; Vrancianu, C.O.; Marinas, I.C.; Popa, M.; Dumbrava, A.S.; Nita-Lazar, M.; Pecete, I.; Muntean, A.A.; Popa, M.I.; et al. Phenotypic and Genotypic Characterization of Recently Isolated Multidrug-Resistant *Acinetobacter baumannii* Clinical and Aquatic Strains and Demonstration of Silver Nanoparticle Potency. *Microorganisms* **2023**, *11*, 2439. [[CrossRef](#)]
19. Jacquemin, D.; Preat, J.; Wathélet, V.; Fontaine, M.; Perpete, E.A. Thioindigo Dyes: Highly Accurate Visible Spectra with TD-DFT. *J. Am. Chem. Soc.* **2006**, *128*, 2072–2083. [[CrossRef](#)]
20. Volkov, V.V.; Chelli, R.; Righini, R.; Perry, C.C. Indigo chromophores and pigments: Structure and dynamics. *Dye. Pigment.* **2020**, *172*, 107761. [[CrossRef](#)]
21. Spoiala, A.; Ilie, C.I.; Dolete, G.; Petrisor, G.; Trusca, R.D.; Motelica, L.; Ficaï, D.; Ficaï, A.; Oprea, O.C.; Ditu, M.L. The Development of Alginate/Ag NPs/Caffeic Acid Composite Membranes as Adsorbents for Water Purification. *Membranes* **2023**, *13*, 591. [[CrossRef](#)]
22. Scientific, T. *Thermo Scientific Evolution 300 UV-Vis Spectrophotometer*; Thermo Electron Scientific Instruments LLC.: Madison, WI, USA, 2013; pp. 1–16.
23. Motoc, A.M.; Valsan, S.; Slobozeanu, A.E.; Corban, M.; Valerini, D.; Prakasam, M.; Botan, M.; Dragut, V.; Vasile, B.S.; Surdu, A.V.; et al. Design, Fabrication, and Characterization of New Materials Based on Zirconia Doped with Mixed Rare Earth Oxides: Review and First Experimental Results. *Metals* **2020**, *10*, 746. [[CrossRef](#)]
24. Boden, A.C.; Bhave, M.; Cipolla, L.; Kingshott, P. Solution deposition conditions influence the surface properties of 3-mercaptopropyl (trimethoxysilane) (MPTS) films. *Appl. Surf. Sci.* **2022**, *602*, 154282. [[CrossRef](#)]
25. Chen, W.-H.; Tseng, Y.-T.; Hsieh, S.; Liu, W.-C.; Hsieh, C.-W.; Wu, C.-W.; Huang, C.-H.; Lin, H.-Y.; Chen, C.-W.; Lin, P.-Y.; et al. Silanization of Solid Surfaces via Mercaptopropylsilatrane: A New Approach of Constructing Gold Colloid Monolayers. *R. Soc. Chem.* **2010**, *4*, 46527–46535. [[CrossRef](#)]
26. Mansur, H.; Oréface, R.; Pereira, M.; Lobato, Z.; Vasconcelos, W.; Machado, L. FTIR and UV-vis study of chemically engineered biomaterial surfaces for protein immobilization. *Spectroscopy* **2002**, *16*, 351–360. [[CrossRef](#)]
27. Chen, M.-A.; Lu, X.-B.; Guo, Z.-H.; Huang, R. Influence of hydrolysis time on the structure and corrosion protective performance of (3-mercaptopropyl)triethoxysilane film on copper. *Corros. Sci.* **2011**, *53*, 2793–2802. [[CrossRef](#)]
28. Piwoński, I.; Grobelny, J.; Cichowski, M.; Celichowski, G.; Rogowski, J. Investigation of 3-mercaptopropyltrimethoxysilane self-assembled monolayers on Au(111) surface. *Appl. Surf. Sci.* **2005**, *242*, 147–153. [[CrossRef](#)]
29. Sakai, T.; Enomoto, H.; Sakai, H.; Abe, M. Direct Fabrication of Silica-Coated Gold Nanoparticles and Gold Nanoparticle-Deposited Silica Spheres in Aqueous Media. *J. Jpn. Soc. Colour Mater.* **2009**, *82*, 387–396. [[CrossRef](#)]

30. Lee, S.; Lee, J. Antibacterial Coating of Glass Fiber Filters with Silver Nanoparticles (AgNPs) and Glycidyltrimethylammonium Chloride (GTAC). *Fiber Polym.* **2018**, *19*, 2080–2087. [[CrossRef](#)]
31. Suntako, R. Effect of Modified Silica Fume Using MPTMS for the Enhanced EPDM Foam Insulation. *Polymers* **2021**, *13*, 2996. [[CrossRef](#)]
32. Marrone, M.; Montanari, T.; Busca, G.; Conzatti, L.; Costa, G.; Castellano, M.; Turturro, A. A Fourier Transform Infrared (FTIR) Study of the Reaction of Triethoxysilane (TES) and Bis [3-triethoxysilylpropyl]tetrasulfane (TESPT) with the Surface of Amorphous Silica. *J. Phys. Chem. B* **2004**, *108*, 3563–3572. [[CrossRef](#)]
33. Chakrabarti, S.; Dutta, B.K. On the adsorption and diffusion of Methylene Blue in glass fibers. *J. Colloid. Interface Sci.* **2005**, *286*, 807–811. [[CrossRef](#)] [[PubMed](#)]
34. Chandio, Z.A.; Talpur, F.N.; Khan, H.; Afridi, H.I.; Khaskheli, G.Q. Determination of cadmium and zinc in vegetables with online FAAS after simultaneous pre-concentration with 1,5-diphenylthiocarbazone immobilised on naphthalene. *Food Addit. Contam. Part. A* **2013**, *30*, 110–115. [[CrossRef](#)] [[PubMed](#)]
35. Huda, B.N.; Wahyuni, E.T.; Mudasir, M. Eco-friendly immobilization of dithizone on coal bottom ash for the adsorption of lead (II) ion from water. *Results Eng.* **2021**, *10*, 100221. [[CrossRef](#)]
36. Ibrahim, M.; El-Nahass, M.M.; Kamel, M.A.; El-Barbary, A.A.; Wagner, B.D.; El-Mansy, M.A. On the spectroscopic analyses of thioindigo dye. *Spectrochim. Acta A Mol. Biomol. Spectrosc.* **2013**, *113*, 332–336. [[CrossRef](#)]
37. Pallavicini, P.; Bassi, B.; Chirico, G.; Collini, M.; Dacarro, G.; Fratini, E.; Grisoli, P.; Patrini, M.; Sironi, L.; Taglietti, A.; et al. Modular approach for bimodal antibacterial surfaces combining photo-switchable activity and sustained biocidal release. *Sci. Rep.* **2017**, *7*, 5259. [[CrossRef](#)]
38. Al-Sakkaf, M.K.; Basfer, I.; Iddrisu, M.; Bahadi, S.A.; Nasser, M.S.; Abussaud, B.; Drmosh, Q.A.; Onaizi, S.A. An Up-to-Date Review on the Remediation of Dyes and Phenolic Compounds from Wastewaters Using Enzymes Immobilized on Emerging and Nanostructured Materials: Promises and Challenges. *Nanomaterials* **2023**, *13*, 2152. [[CrossRef](#)]
39. Doveri, L.; Taglietti, A.; Grisoli, P.; Pallavicini, P.; Dacarro, G. Dual mode antibacterial surfaces based on Prussian blue and silver nanoparticles. *Dalton Trans.* **2023**, *52*, 452–460. [[CrossRef](#)]

Disclaimer/Publisher's Note: The statements, opinions and data contained in all publications are solely those of the individual author(s) and contributor(s) and not of MDPI and/or the editor(s). MDPI and/or the editor(s) disclaim responsibility for any injury to people or property resulting from any ideas, methods, instructions or products referred to in the content.